

Understanding elemental anomalies in Globular Clusters: Experimental study of the $^{30}\text{Si}(p,\gamma)^{31}\text{P}$ reaction

Djamila Sarah HARROUZ

Supervisors:
Nicolas de Séréville
Faïrouz Hammache

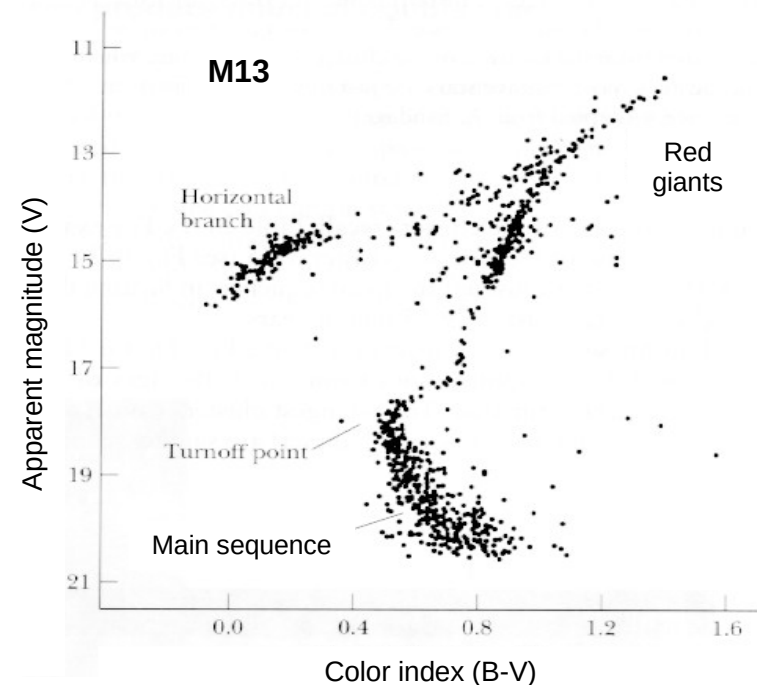
université
PARIS-SACLAY

XXIInd Colloque Ganil
28th septembre 2021

 IJCLab
Irène Joliot-Curie
Laboratoire de Physique
des 2 Infinis

Globular Clusters

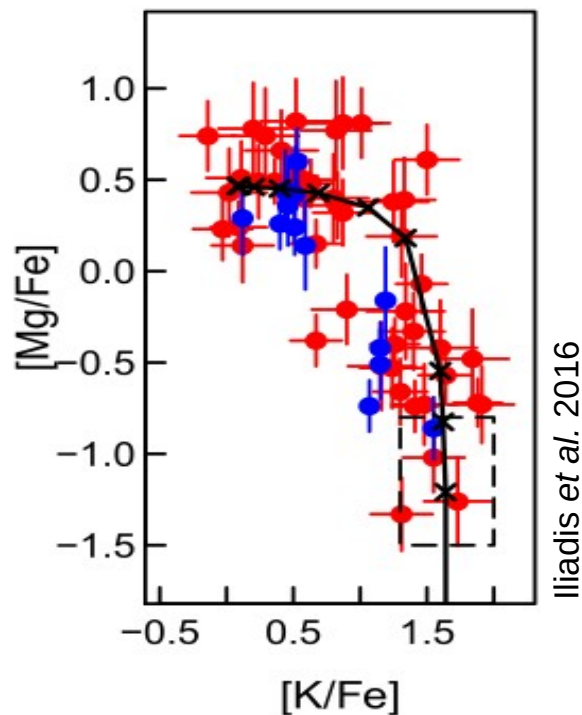
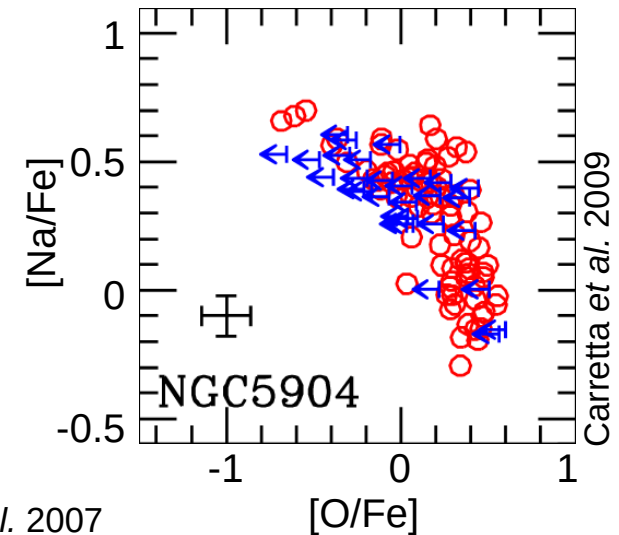
- Gravitationally bound systems of 10^5 to 10^7 stars, located in halo of spiral galaxies.
- Among the oldest structures in the Universe (age > 10 Gyr).
- Globular Clusters are important for:
 - Cosmology (age of the Universe)
 - Galactic physics (formation and early evolution of galaxies)
- Low mass stars mainly on the **Main Sequence** and **Red Giant** branch.
 - Hydrogen-burning
- Paradigm: **Single stellar population**: same age and chemical composition.



Abundance anomalies in Globular Clusters

- Spectroscopic observations in Red Giant stars:
 - Abundance anticorrelation for **C-N, O-Na, Mg-Al**
 - Abundances vary from star-to-star
- Red giant stars temperature too low to alter abundances
 - Abundances partially inherited from **unknown stars from previous generation, called polluters.**

Polluters must burn Hydrogen at $T \sim 75$ MK (Prantzos *et al.* 2007 & 2017)

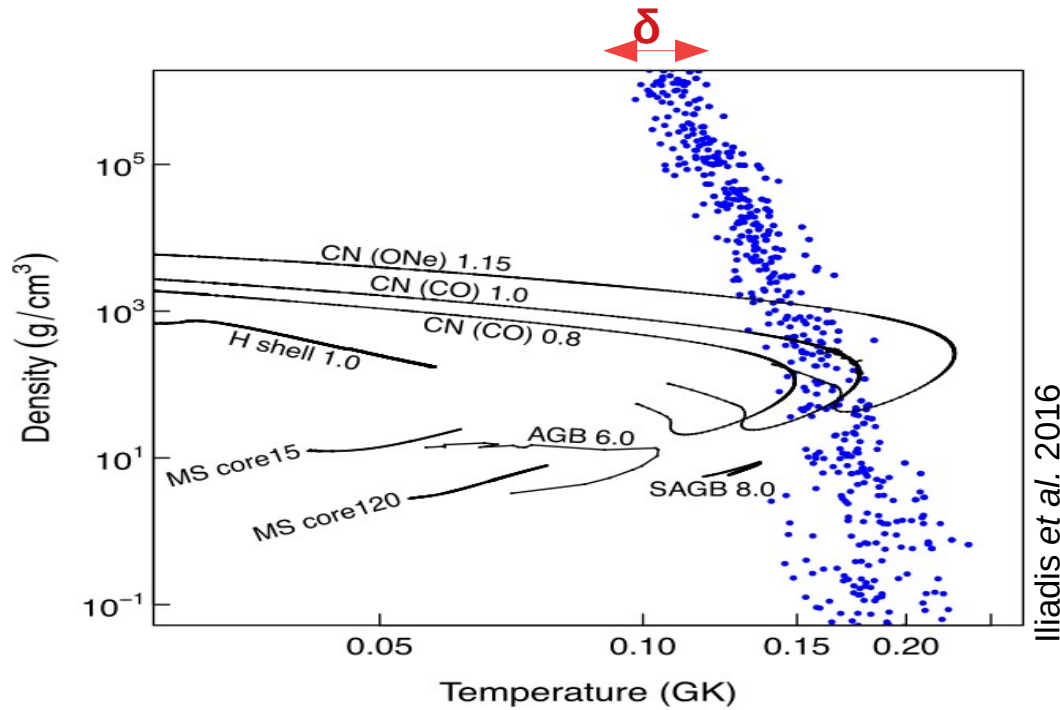


Extreme case of NGC 2419

- Observed **Mg-K** anticorrelation
- Requires much higher temperature in polluter site (between 100 MK and 200 MK) to overcome Coulomb barrier in proton capture reactions.

What is the nature and type of polluter stars? (T, ρ)?

NGC2419 Abundances

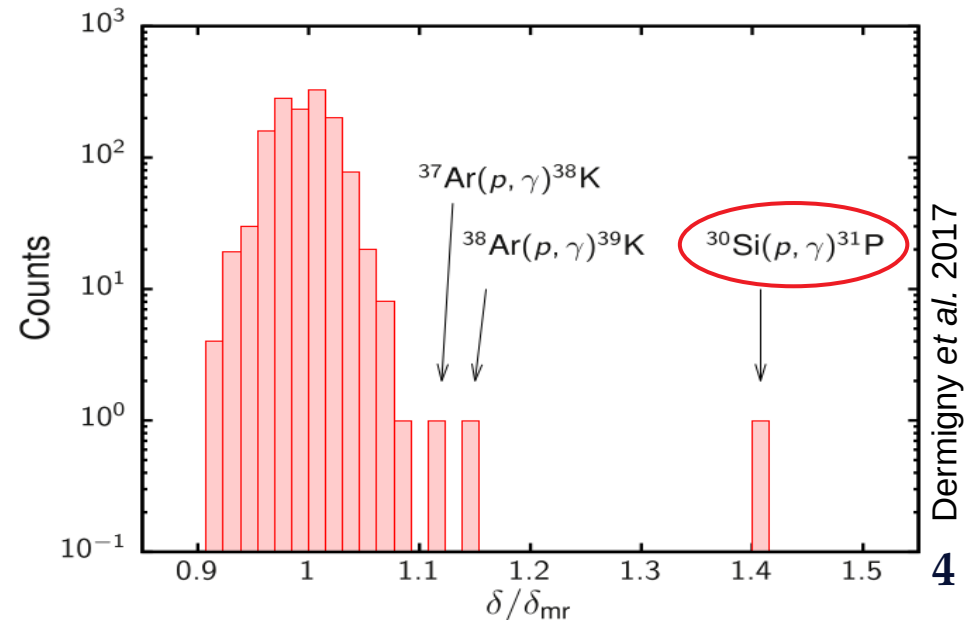


Key Reactions

- Individual variation of reaction rates within their uncertainties.
- Impact of a few (p,γ) reactions.
- $^{30}\text{Si}(p,\gamma)^{31}\text{P}$ reaction contributes the most to the spread of the (T, ρ) locus for $100 \text{ MK} < T < 200 \text{ MK}$

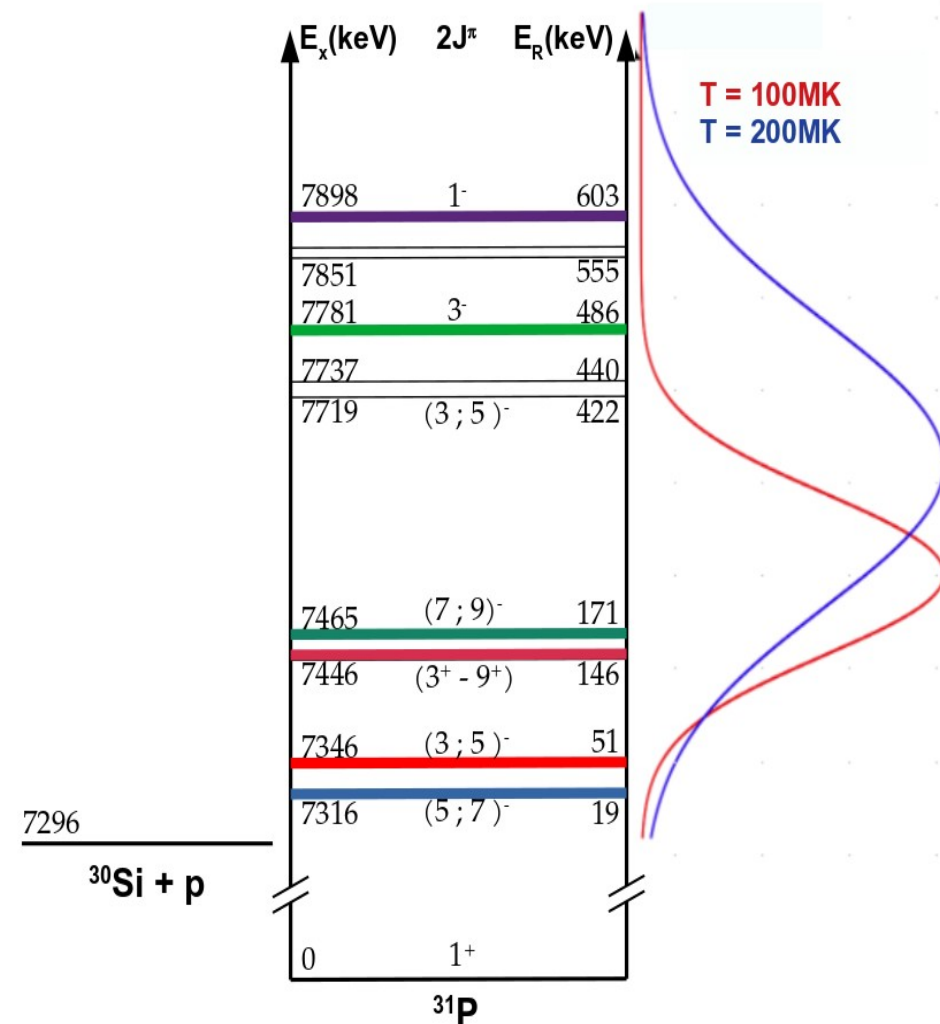
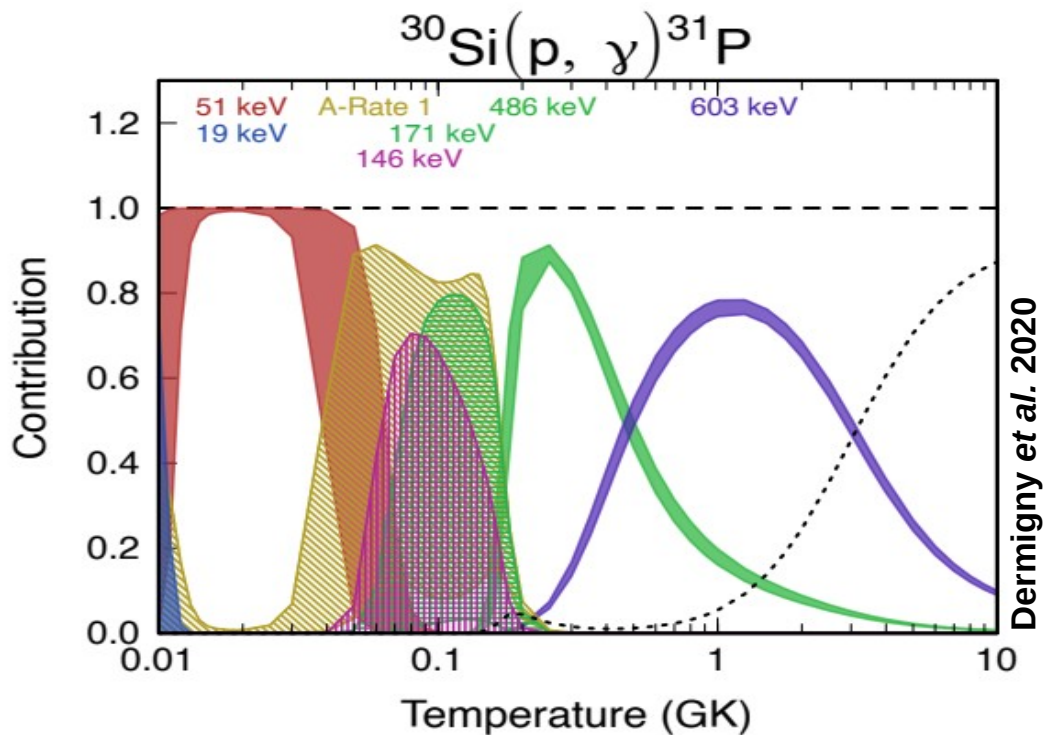
Sensitivity Studies

- Simulate nucleosynthesis reaction network in **H-burning conditions** (with Monte Carlo calculation) for uniform **T** and **ρ** distributions, and varying reaction rates within uncertainties.
- Uncertainty on reaction rates → T spread increased by 70%.



State of the art for $^{30}\text{Si}(p,\gamma)^{31}\text{P}$ reaction

- Energies known with uncertainty better than 4 keV
- Spins and parities constrained but mostly unknown



- $E_r = 19$ keV: $C^2S = 0.002$ (Vernotte et al. 1990)
- $E_r = 51$ and 146 keV: Mean reduced widths, systematic study $\langle \theta^2 \rangle = 0.0003$
- $E_r = 171$ keV: Upper limit $C^2S < 0.003$ (Dermigny et al. 2020)

- $E_r = 422, 486$ keV sole direct measurements using $\gamma\gamma$ coincidences (Dermigny et al. 2020)
- $E_r = 603$ keV: several direct measurements, reference resonance

Experimental Strategy

Thermonuclear reaction rate for single and isolated narrow resonance :

$$\langle \sigma v \rangle \propto (\omega\gamma) e^{-E_R/kT}$$

$$\omega\gamma = \frac{2J_R + 1}{(2J_p + 1)(2J_{30Si} + 1)} \frac{\Gamma_p \Gamma_\gamma}{\Gamma}$$

High energy

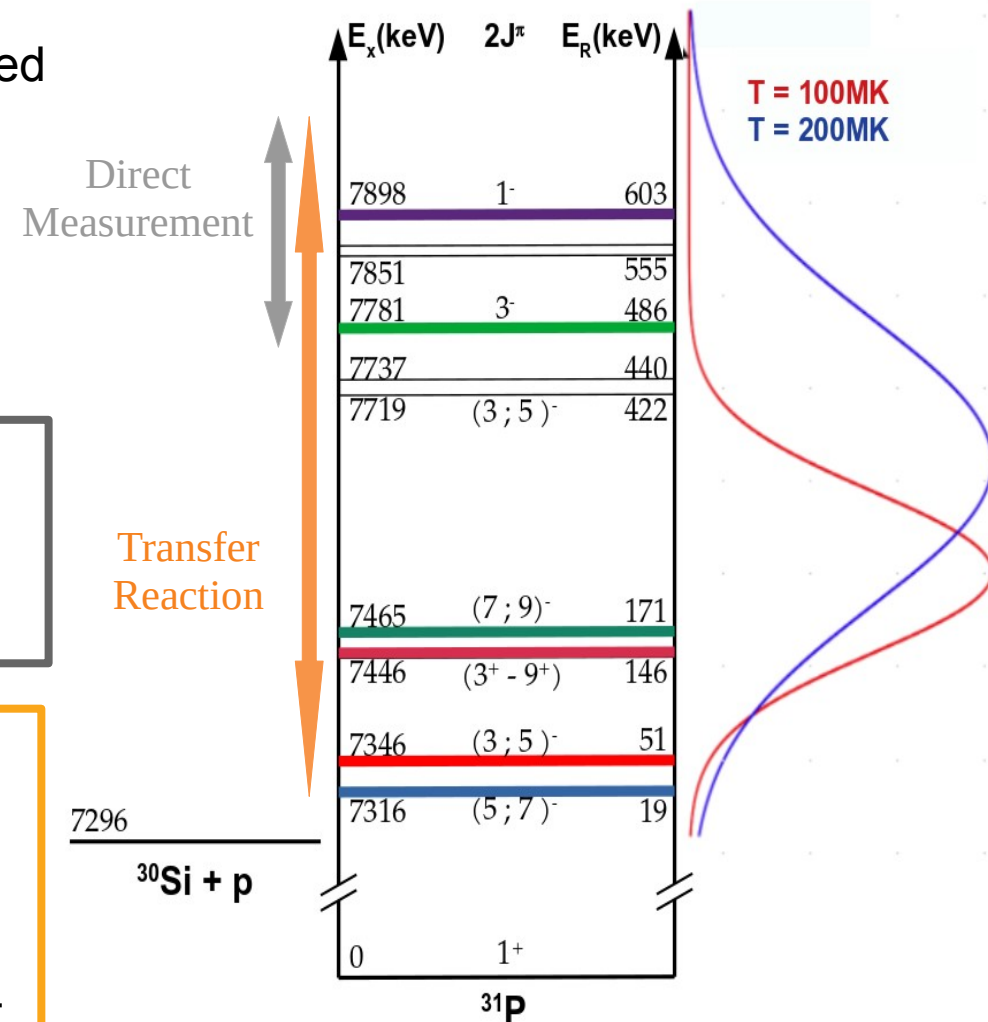
- Direct measurement of resonance strength $\omega\gamma$ @DRAGON (Triumf)
- Independent strength determination of the 484 keV resonance.

Low energy

$$\begin{cases} \Gamma = \Gamma_p + \Gamma_\gamma \\ \Gamma_p \ll \Gamma_\gamma \end{cases} \implies \omega\gamma \simeq \omega\Gamma_p$$

$^{30}\text{Si}(^3\text{He},d)^{31}\text{P}$ transfer reaction

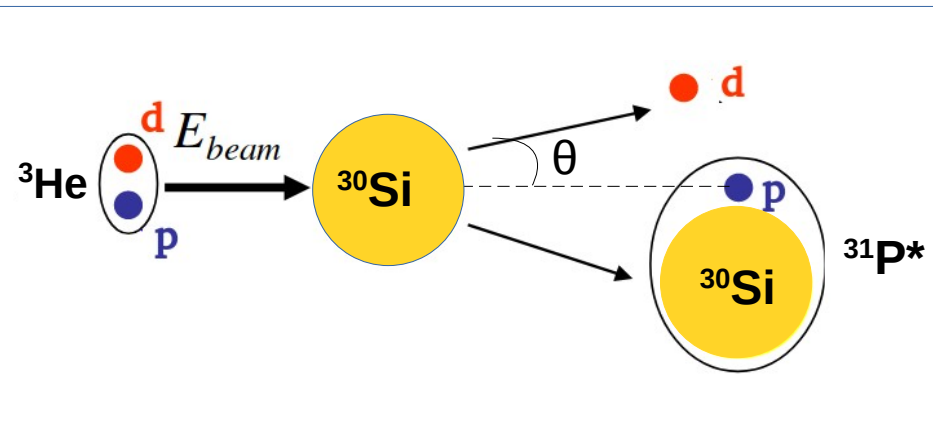
- Experiment by Vernotte in 1990 at Orsay's SplitPole: low statistics, limited resolution and contaminations.
- → new measurements @Q3D (MLL) with improved energy resolution and sensitivity.



One proton Transfer Reaction

(p,γ) can be studied through one proton (³He,d) transfer reaction

Experimental method



Theoretical model for direct transfer

Distorted Wave Born Approximation:

- Elastic scattering dominates entrance and exit channels (described by optical models)
- Transfer 1st order perturbation
- No configuration rearrangement

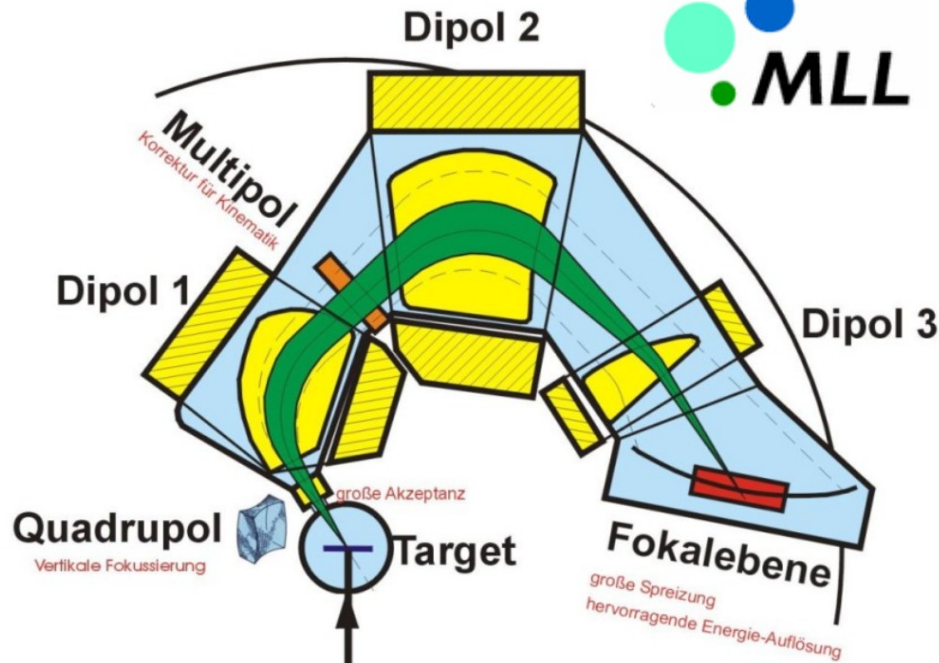
- Excitation energies

• Angular distribution → $\frac{d\sigma}{d\Omega}(\theta)_{exp} = C^2 S \frac{d\sigma}{d\Omega}(\theta)_{DWBA}$

$$\Gamma_p = C^2 S \Gamma_p^{s.p}(E_r, \ell)$$

- Shape of the distribution
→ transferred angular orbital momentum ℓ

$^{30}\text{Si}(^3\text{He},d)^{31}\text{P}$ reaction @Q3D



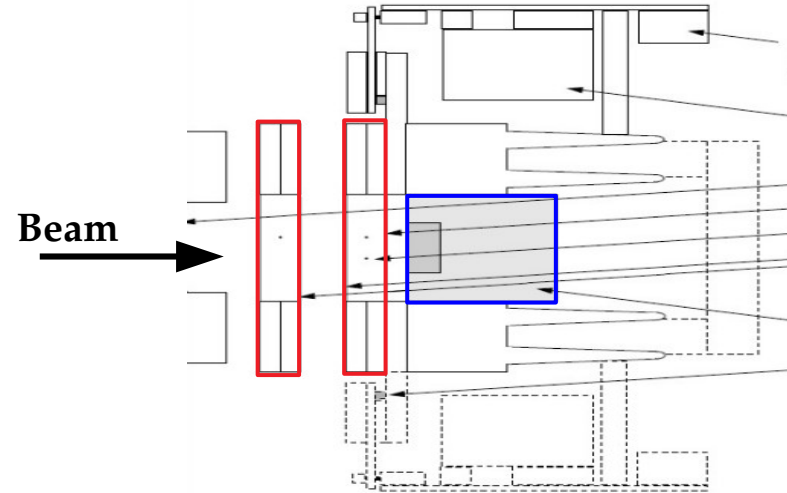
Beam ^3He : $E = 25 \text{ MeV}$
 $I = 200 \text{ nAe}$

Targets: $^{30}\text{SiO}_2$ ($40 \mu\text{g}/\text{cm}^2$) enriched at 95% on ^{nat}C
 $^{nat}\text{SiO}_2$ ($20 \mu\text{g}/\text{cm}^2$) on ^{nat}C

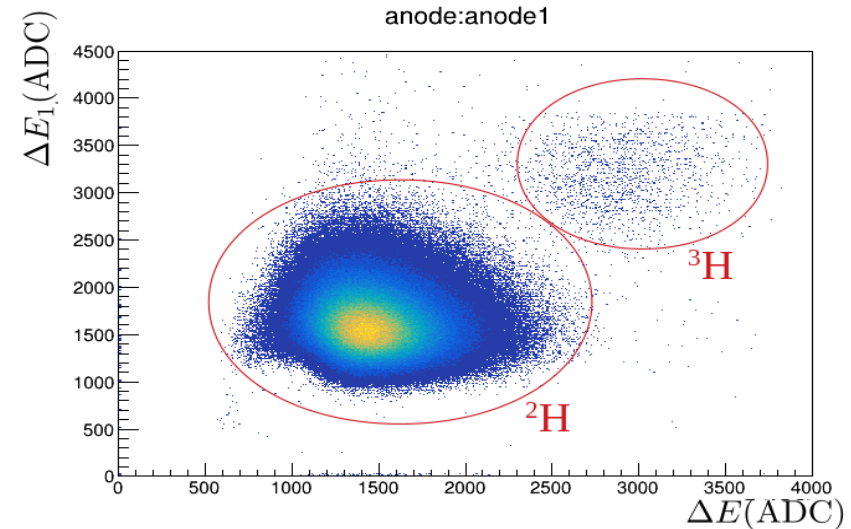
Solid Angle : 4 to 12 msr

Energy resolution $\frac{\Delta E}{E} \sim 2 \cdot 10^{-4}$

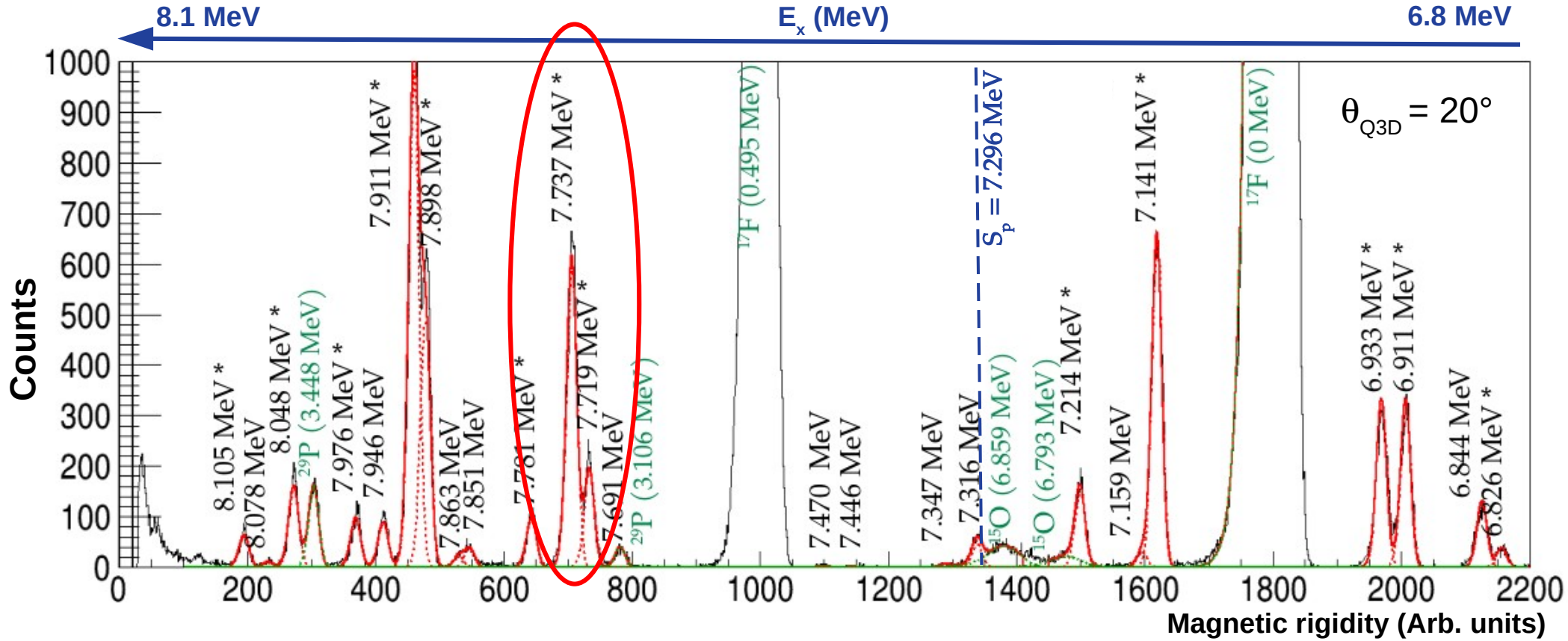
Focal plane detectors :



- **Single-wire proportional counters** → position on the focal plane and energy loss.
- **Plastic scintillator** → residual energy.



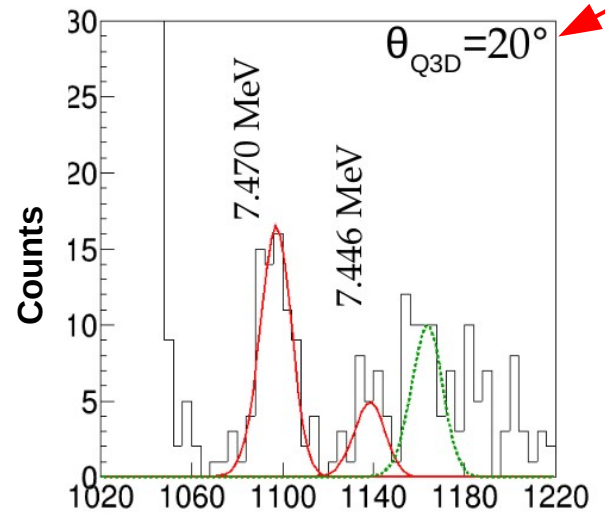
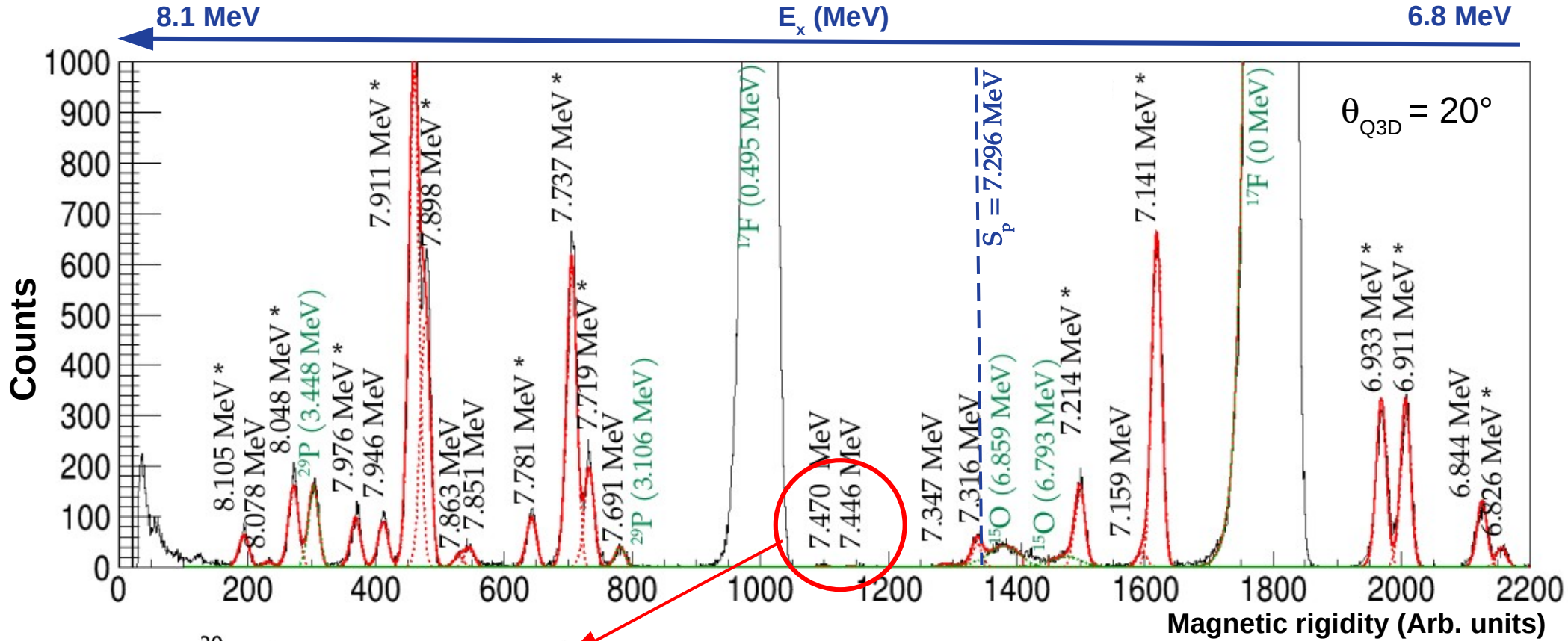
Magnetic rigidity spectrum



- Spectra for 7 lab angles : 6°, 10°, 12°, 16°, 20°, 23°, 32°
- Fit with multiple skewed gaussians with common width.
- Experimental resolution **FWHM ~ 7 keV**
Vernotte (1990) ~25 keV

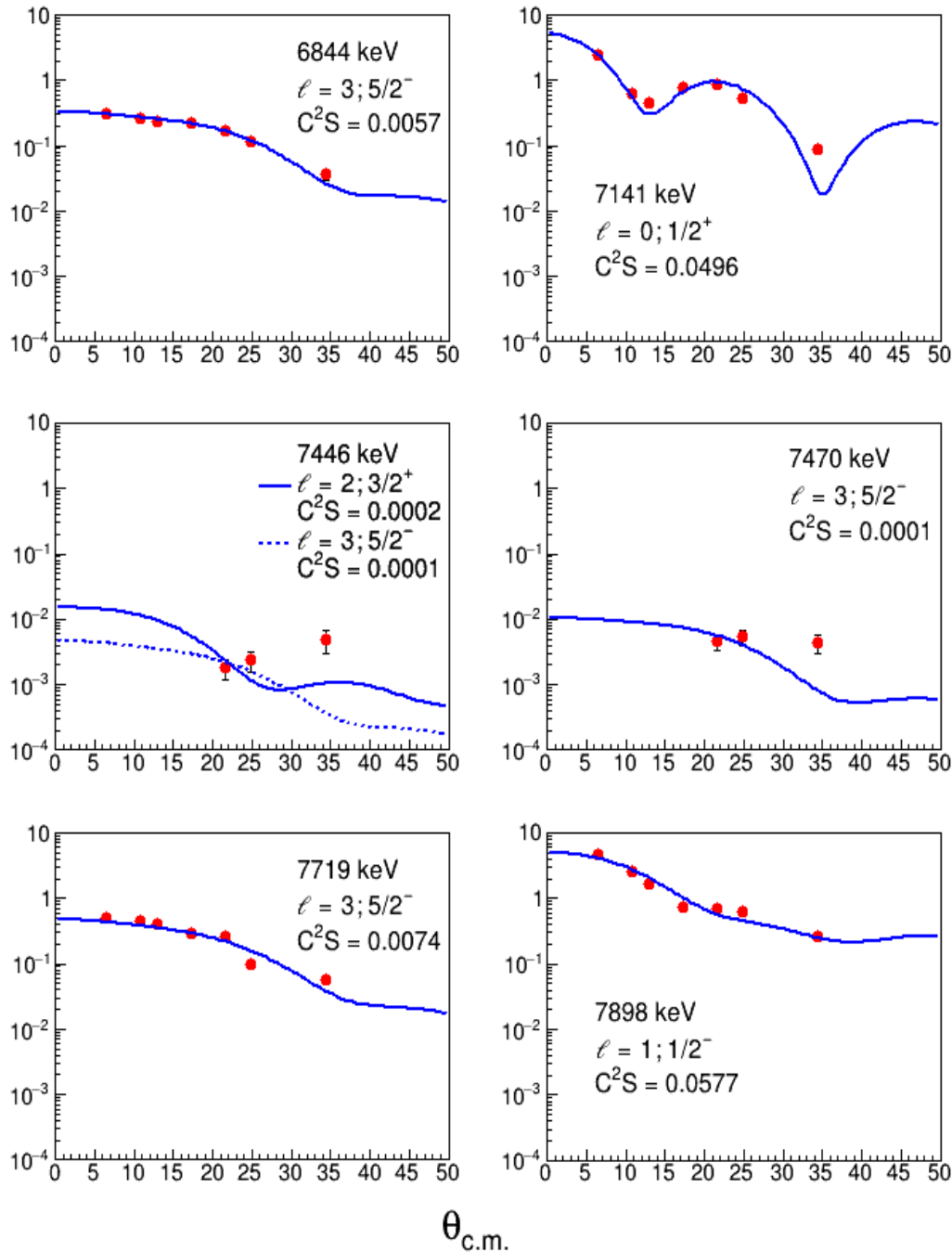
- Doublet at $E_x = 7719 - 7737$ keV separated.

Magnetic rigidity spectrum



- Doublet at $E_x = 7719 - 7737$ keV separated.
- Levels at $E_x = 7446$ and 7470 keV observed for $\theta_{Q3D} \geq 20^\circ$.

Angular distributions



Differential cross section

$$\frac{d\sigma}{d\Omega}(\theta_{c.m.})_{exp} = \frac{N_d(\theta_{c.m.})}{N_{beam}N_{target}\Delta\Omega_{c.m.}} = C^2S \frac{d\sigma}{d\Omega}(\theta_{c.m.})_{DWBA}$$

Finite-Range DWBA calculations

→ performed with **FRESCO** code.

Optical potentials

$^{30}\text{Si} + ^3\text{He}$: Vernotte et al (1982)

$^{31}\text{P} + d$: Daehnick, (1980)

Binding Potentials

$^{30}\text{Si} + p$: Wood-Saxon, volume + Spin-Orbit

$\langle ^3\text{He} | d+p \rangle$ overlap: GFMC Brida (2011)

→ C^2S extrapolated to correct unbound energy

$$\Gamma_p \propto C^2S |R(r)|^2 \quad r = 7fm$$

Radial wave-function calculation

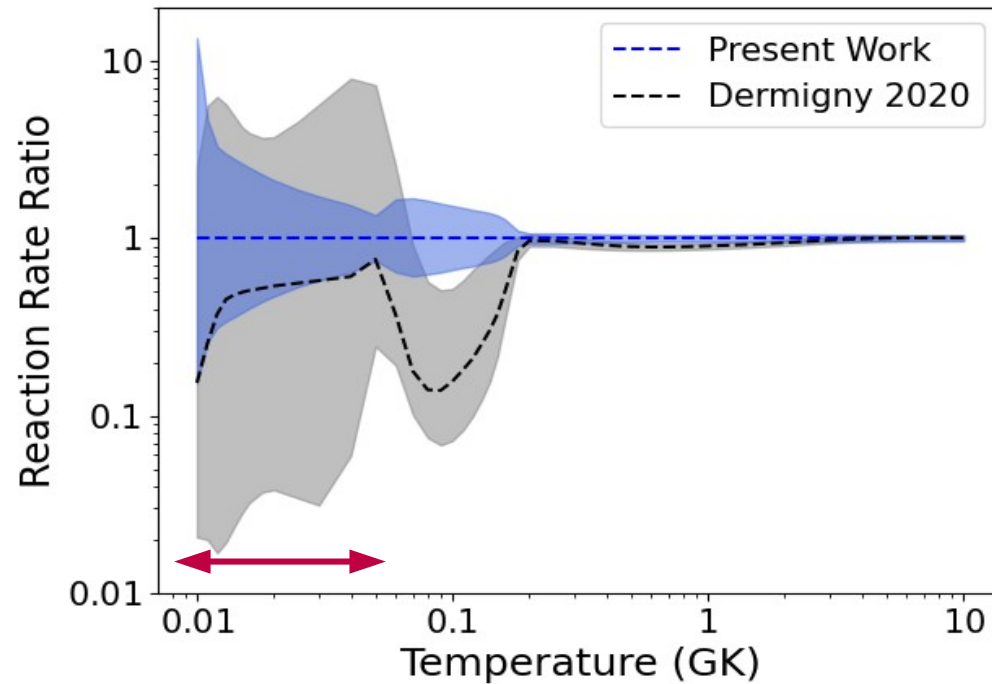
→ performed with **DWUCK4** code

Vincent & Fortune (1970) procedure

• Γ_p uncertainties ~ 30% (from optical pot.)

$^{30}\text{Si}(p,\gamma)^{31}\text{P}$ Reaction Rate

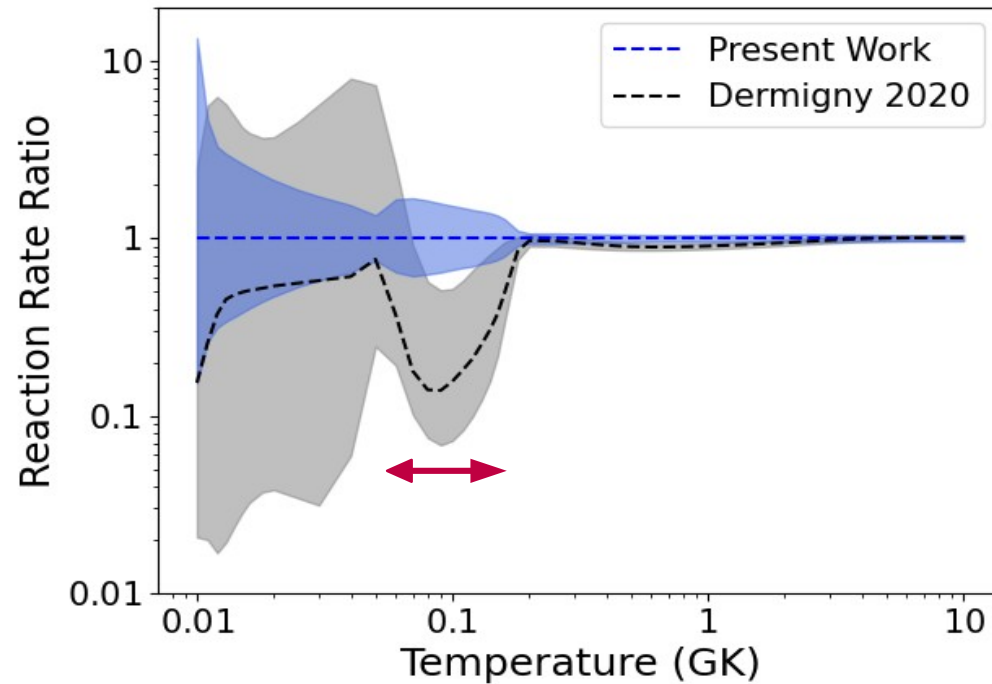
- Monte Carlo calculations using **RatesMC**.
- 68% uncertainty bands (log-normal distribution)



- Determination of C²S for $E_r = 19$ keV, $E_r = 51$ keV and $E_r = 170$ keV (previously upper limits)

$^{30}\text{Si}(p,\gamma)^{31}\text{P}$ Reaction Rate

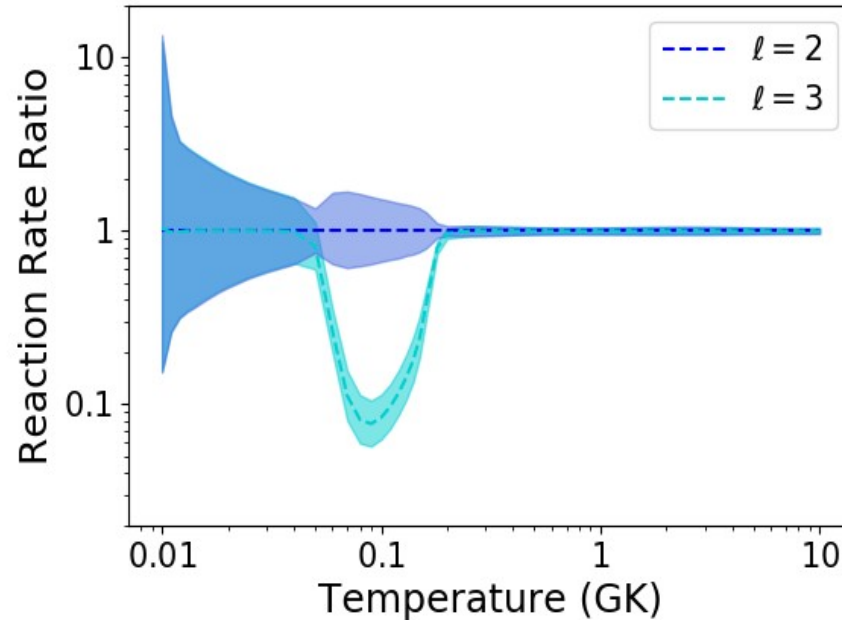
- Monte Carlo calculations using **RatesMC**.
- 68% uncertainty bands (log-normal distribution)



- Determination of C^2S for $E_r = 19$ keV, $E_r = 51$ keV and $E_r = 170$ keV (previously upper limits)
- Observation of the $E_r = 149$ keV → **key resonance** in $T = 100\text{-}200$ MK

$^{30}\text{Si}(p,\gamma)^{31}\text{P}$ Reaction Rate

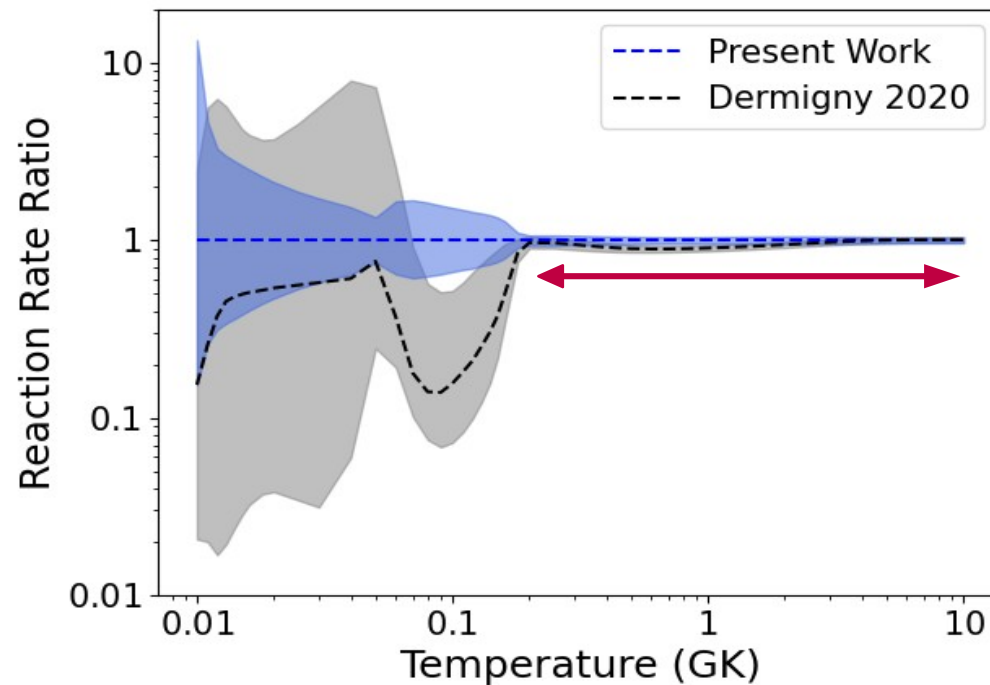
- Monte Carlo calculations using **RatesMC**.
- 68% uncertainty bands (log-normal distribution)



- Determination of C²S for $E_r = 19$ keV, $E_r = 51$ keV and $E_r = 170$ keV (previously upper limits)
- Observation of the $E_r = 149$ keV → **key resonance** in $T = 100$ - 200 MK
→ $\ell = 2$ or $\ell = 3$, induces a factor of 10 difference in the reaction rate
→ **spin/parity have to be better constrained!**

$^{30}\text{Si}(p,\gamma)^{31}\text{P}$ Reaction Rate

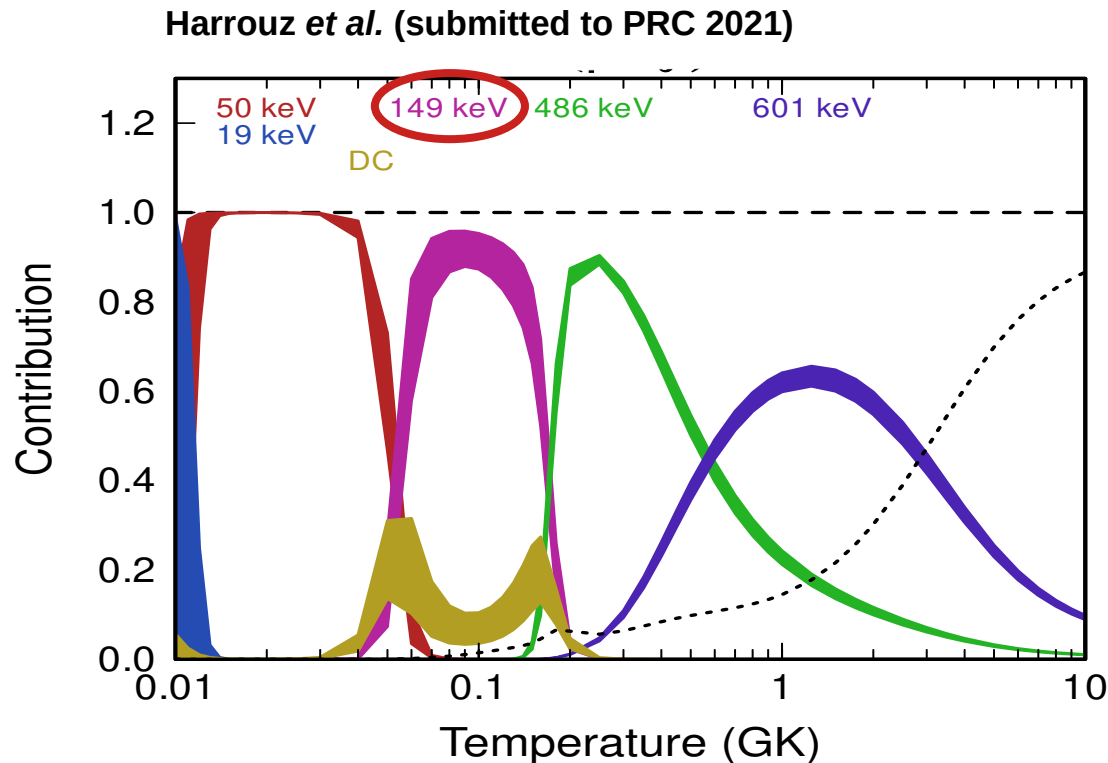
- Monte Carlo calculations using **RatesMC**.
- 68% uncertainty bands (log-normal distribution)



- Determination of C²S for $E_r = 19$ keV, $E_r = 51$ keV and $E_r = 170$ keV (previously upper limits)
- Observation of the $E_r = 149$ keV → **key resonance** in $T = 100$ - 200 MK
- → $\ell = 2$ or $\ell = 3$, induces a factor of 10 difference in the reaction rate
→ **spin/parity have to be better constrained!**
- $E_r = 418 - 440$ keV doublet resolved → $E_r = 418$ keV has $\ell=3$, negligible contribution to the reaction rate, in agreement with direct measurements (*Dermigny et al. 2020*)
- $E_r = 486$ keV: good agreement for strength values (within 30%) with direct measurements.

Conclusion

- Extraction of spectroscopic information for the ^{31}P nucleus between $E_x = 6800 - 8100$ keV from the $^{30}\text{Si}(^3\text{He},d)^{31}\text{P}$ reaction.
- Calculation of strengths for resonances up to $E_r = 600$ keV.
- Improved determination of the $^{30}\text{Si}(p,\gamma)^{31}\text{P}$ reaction rate.
- Evincing the importance of key resonance at $E_r = 149$ keV → **need to determine its spin/parity**

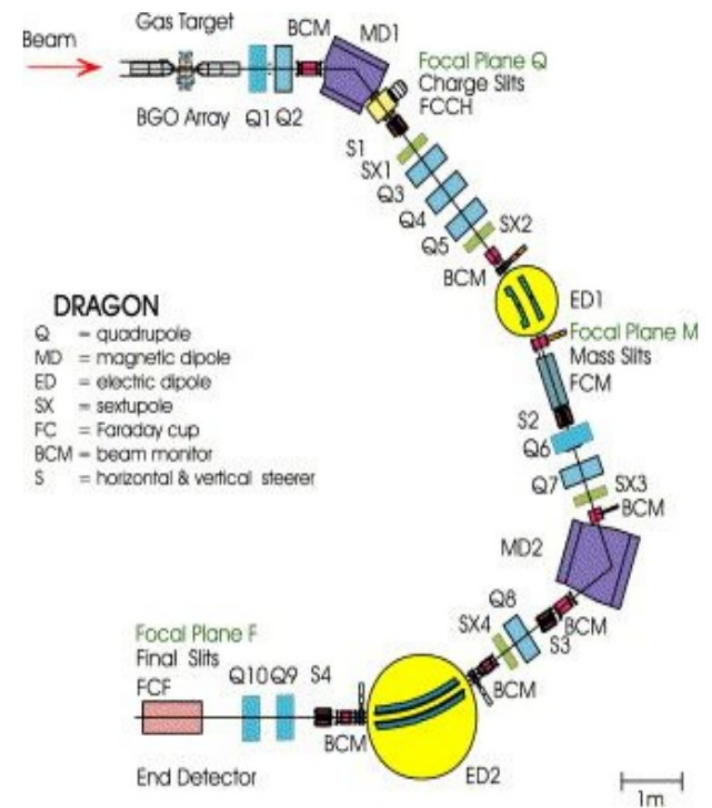
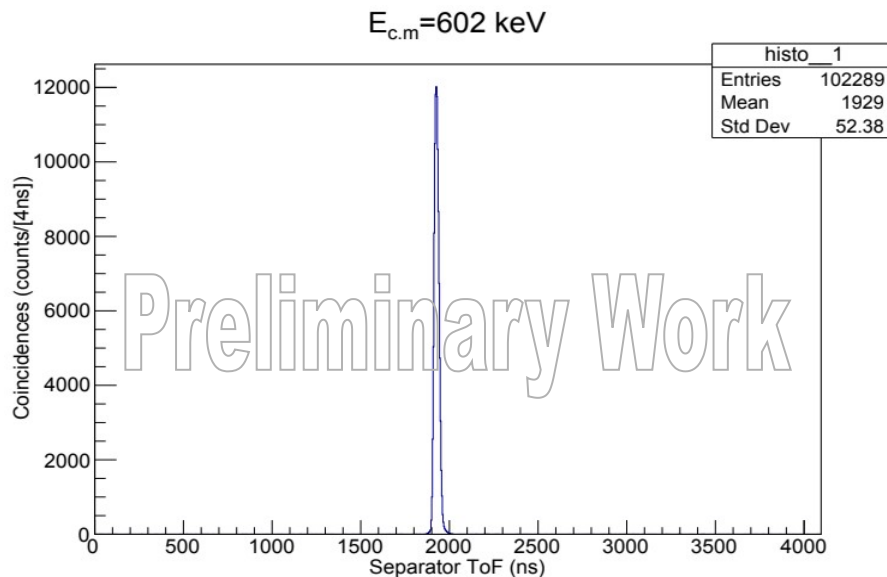


Conclusion

- Extraction of spectroscopic information for the ^{31}P nucleus between $E_x = 6800 - 8100$ keV from the $^{30}\text{Si}(^3\text{He},d)^{31}\text{P}$ reaction.
- Calculation of strengths for resonances up to $E_r = 600$ keV.
- Improved determination of the $^{30}\text{Si}(p,\gamma)^{31}\text{P}$ reaction rate.
- Evincing the importance of key resonance at $E_r = 149$ keV \rightarrow need to determine its spin/parity

Perspectives

- Analysis of the $^{30}\text{Si}(p,\gamma)^{31}\text{P}$ reaction rate with the Recoil spectrometer **DRAGON**



Conclusion

- Extraction of spectroscopic information for the ^{31}P nucleus between $E_x = 6800 - 8100$ keV from the $^{30}\text{Si}(^3\text{He},d)^{31}\text{P}$ reaction.
- Calculation of strengths for resonances up to $E_r = 600$ keV.
- Improved determination of the $^{30}\text{Si}(p,\gamma)^{31}\text{P}$ reaction rate.
- Evincing the importance of key resonance at $E_r = 149$ keV \rightarrow need to determine its spin/parity

Perspectives

- Analysis of the $^{30}\text{Si}(p,\gamma)^{31}\text{P}$ reaction rate with the Recoil spectrometer **DRAGON**
- Investigate the impact of the new measurements on the temperature locus for constraining “the polluter” candidates in **Globular Clusters**.





Thank you for your attention

Collaborators :

Philip Adsley (iThemba)

Beyhan Bastin (GANIL)

Thomas Fastermann (TUM)

Fairouz Hammache (IJCLab)

Ralf Hertenberg (TUM)

Marco La Cognata (LNS)

Livio Lamia (LNS)

Richard Longlond (aNCSU / TUNL)

Anne Meyer (IJCLab)

Sara Palmerini (LNS)

Gianluca Pizzone (LNS)

Stefano Romano (LNS)

Nicolas de Séréville (IJCLab)

Aurora Tumino (LNS)

Hans-Friedrich Wirth (TUM)